Structure of expanded fluid Rb and Cs: a quantum molecular dynamics study

2006 J. Phys.: Condens. Matter 18 5597

(http://iopscience.iop.org/0953-8984/18/24/002)

INSTITUTE OF PHYSICS PUBLISHING JOURNAL OF PHYSICS: CONDENSED MATTER

J. Phys.: Condens. Matter **18** (2006) 5597–5605 doi:10.1088/0953-8984/18/24/002

Structure of expanded fluid Rb and Cs: a quantum molecular dynamics study

A Kietzmann[1], R Redmer[1], F Hensel[2], M P Desjarlais[3] and T R Mattsson[3]

[1] Institut für Physik, Universität Rostock, D-18051 Rostock, Germany
[2] Fachbereich Chemie, Philipps-Universität Marburg, Postfach, D-35032 Marburg, Germany
[3] Pulsed Power Sciences Center, Sandia National Laboratories, Albuquerque, NM 87185, USA

Received 22 December 2005, in final form 19 March 2006
Published 2 June 2006
Online at stacks.iop.org/JPhysCM/18/5597

Abstract

We have performed quantum molecular dynamics simulations for expanded fluid Rb and Cs. We compare the pair correlation functions with results derived from neutron and x-ray scattering experiments. The experimentally observed structural changes with the density and temperature variation are reproduced. The density of states and the electronic charge density extracted from the simulations indicate a crossover from metallic to nonmetallic behaviour near the critical point due to a localization of electrons at nuclei.

1. Introduction

The physical properties of fluid alkali metals and mercury have been studied intensively both experimentally and theoretically [1]. The most interesting feature in fluid metals compared with Lennard-Jones systems is the density dependence of the interaction potential between the charged particles. This leads to a strong state dependence of the thermodynamic properties and to a metal-to-nonmetal transition which occurs just in the vicinity of the critical point of the liquid–vapour phase transition. The simultaneous electronic and thermodynamic transitions give rise to a number of unique features in the physical properties of fluid metals such as the asymmetry of their coexistence curves, an enhancement of the paramagnetic spin susceptibility in the expanded fluid range, or the change of sign of the thermopower near the critical point; for a review, see [1].

The structural changes in the fluid when thermally expanded from the melting to the critical point were measured in pioneering neutron scattering experiments (Cs) [2, 3] and high-precision x-ray diffraction experiments (Rb) [4]. These experiments indicate a continuous crossover from a metallic fluid characterized by the short-ranged, screened Coulomb interaction near and above the melting point to an atomic vapour with a Lennard-Jones-type pair potential. The respective metal-to-nonmetal transition is a result of the relocalization of free conduction electrons at nuclei with ongoing expansion. Although this qualitative explanation is simple it nevertheless requires the treatment of fundamental problems of many-particle physics such as disorder and correlations for a more detailed description. Furthermore, the dense vapour is not monatomic as in noble gases but consists also of dimers and further neutral and charged clusters

as shown in advanced chemical models; see [5, 6]. A close relation between the decrease of the ionization degree and that of the electrical conductivity along the coexistence curve has been established in such chemical models [7].

However, chemical models require information about the density-dependent ionization energies and cross sections for the scattering of free electrons at ions and atoms. Furthermore, the discrimination between *bound* and *free* electrons becomes questionable near the metal-to-nonmetal transition region.

Alternatively, simulation techniques and integral equation methods based on the physical picture can provide more insight into changes of the electronic binding character and the related physical properties with the density. Classical molecular dynamics studies for liquid alkali metals were performed using pseudopotentials [8, 9] or effective pair potentials which can be derived, for example, from measured static structure data by an *inverse method* [10, 11].

Applying density functional theory (DFT), a set of integral equations for the pair correlation functions in dense plasmas or liquid metals can be derived [12, 13]. This *quantal hypernetted chain* approximation was applied to various systems including compressed liquid Rb [14]. Orbital-free molecular dynamics simulations [15] are based on simple kinetic energy functionals such as the Thomas–Fermi one so that the computational effort is manageable. Therefore, simulations can be performed both for a large number of particles and time steps giving access to the dynamical properties of the system.

On the other hand, state-of-the-art quantum molecular dynamics (QMD) simulations combine advanced electronic structure calculations using DFT with molecular dynamics simulations and are, thus, a powerful tool to treat the static and dynamic properties of Coulomb systems within a strict physical picture; see [16] for a review. QMD simulations require massive parallelization and they have been applied so far for a number of elements such as aluminium [17], copper [18], and hydrogen [19].

The first QMD simulations for expanded liquid Cs and Rb were performed within the Born–Oppenheimer approximation using the local density approximation (LDA) of DFT [20, 21]. Because of the great computational effort only a few (2–3) density–temperature points could be studied at that time; the lowest density considered was still about three times the critical density. Further simulations were performed along the melting line of Rb [22, 23] and compared with experimental data [24]; reasonable agreement has been achieved.

The generalized gradient approximation (GGA) is in general better suited for states near the critical point where inhomogeneities of the electron density are important and the LDA is probably insufficient. One single density–temperature point near the critical point of Rb has been studied within a QMD simulation based on the GGA in order to prove the existence of transient dimers in the liquid phase [25] which are proposed to give the inelastic peak observed in the experimental dynamic structure factor [3]. Instead, transient trimers were identified in these QMD simulations to be responsible for that feature.

In this paper we present the first extensive study of the structural properties of expanded liquid Cs and Rb based on QMD simulations using the GGA of DFT. A large number of points from the melting up to the critical point has been considered which covers almost the whole path of the experiments in the density–temperature plane. We focus on the structural information contained in the pair correlation function but also give results for the changes of the density of states and of the electron density along the expansion which are crucial for the understanding of the metal-to-nonmetal transition.

2. QMD simulations

QMD simulations take advantage of state-of-the-art electronic structure calculations within DFT for a given array of ion positions. Solving the Schrödinger equation for an effective

potential that includes the contribution from the ions, the classical (Hartree) term of the electrons, as well as the quantum-mechanical exchange and correlation contributions, the forces on each ion are computed and a subsequent molecular dynamics step is performed. The repeated application of electronic structure calculations within DFT for a slightly changed array of ion positions and molecular dynamic steps is continued until convergence is reached for the equation-of-state variables (thermodynamic equilibrium).

We have performed *ab initio* molecular dynamics simulations within the framework of Mermin's finite temperature density functional theory (FT-DFT) [26]. The implementation of the QMD method comes from VASP (Vienna *ab initio* simulation package), a plane wave density functional code developed at the University of Vienna [27–30]. To minimize the computational effort we have used the Born–Oppenheimer approximation: only the active electrons, usually corresponding to valence electrons of each atomic species, are treated quantum mechanically on the level of DFT. The electronic wavefunction is relaxed at each QMD step, which assumes decoupled electronic and ionic timescales. We have chosen a simulation box with 64 atoms and periodic boundary conditions; seven active electrons were considered per atom. The core wavefunctions are modelled using the Vanderbilt [31] ultrasoft pseudopotentials (US-PPs) supplied with VASP [32]. These US-PP reduce the computational effort. The exchange–correlation functionals are calculated within the GGA and some with the LDA. Our most accurate calculations were done using the GGA parameterization of Perdew and Wang [33], with a plane wave cutoff E_{cut} at 100 eV. For the representation of the Brillouin zone only the Γ point was used. Calculations for Al have shown that an extension to higher-order **k**-point sets has no significant effect on the results [17].

The particle density in these QMD runs was fixed by the total volume of the cubic supercell. Our simulations were performed for a canonical ensemble with the temperature as a conserved quantity. To hold the temperature at a predefined level, the ion temperature is regulated by a Nosé–Hoover thermostat and the electronic temperature is fixed by Fermi weighting the occupation of bands [29]. The ions are treated classically by the integration of Newton's equations of motion using a fourth-order predictor–corrector algorithm. Using the Hellmann–Feynman theorem the forces on the ions are computed fully quantum mechanically. After about 100 time steps the system was equilibrated and QMD runs with 500–1000 time steps were performed. The time steps were fixed for each QMD run at 10–20 fs depending on the particle density initialized for the system so that the total simulation time was 5–20 ps. The pair correlation functions were calculated by averaging over all equilibrated ion trajectories of a run.

The wavefunctions are expanded in plane waves so that the computational effort increases with decreasing density. For example, a typical QMD run with VASP for Rb or Cs at low densities near the critical point takes about 50 days on a state-of-the-art single workstation. Therefore, it is essential to perform massive parallel calculations to minimize the computational time.

3. Results for the pair correlation function

We show the pair correlation functions $g(r)$ for Cs and Rb for various densities and temperatures along the expansion in figures 1 and 2 and compare with the experimental results. The corresponding coordination numbers N_1 defined by $N_1 = 2\rho \int_0^{R_1} 4\pi r^2 g(r)\,\mathrm{d}r$ and the next-neighbour distances R_1, i.e. the position of the first peak of $g(r)$, are shown in figure 3.

The advantage of this work is the implementation of US-PPs in the GGA. The GGA yields more accurate results for the pair correlation function over wider ranges of density and temperature than the Car–Parrinello method (CP) within the LDA [20]. The problem of

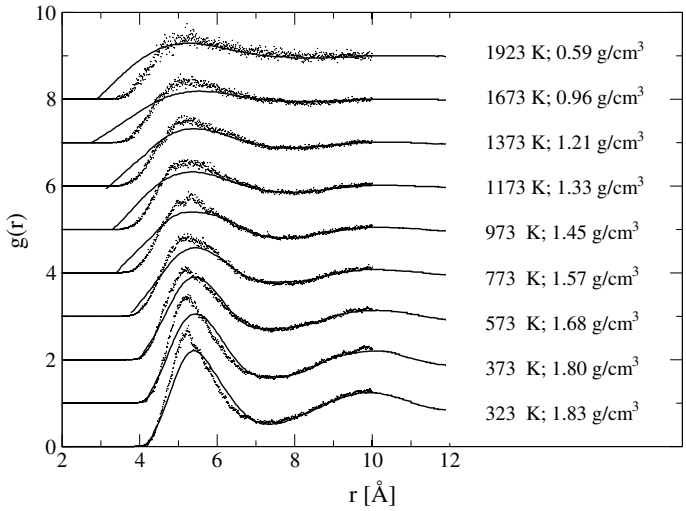

Figure 1. Pair correlation function for expanded fluid Cs: QMD simulations (data points) are compared with neutron scattering experiments (solid lines) [2]. The melting temperature at 1 bar is 301.55 K and the density of the solid is 1.89 g cm^{-3}. The critical point is located at 1924 K, 0.379 g cm^{-3}, and 92.5 bar [34].

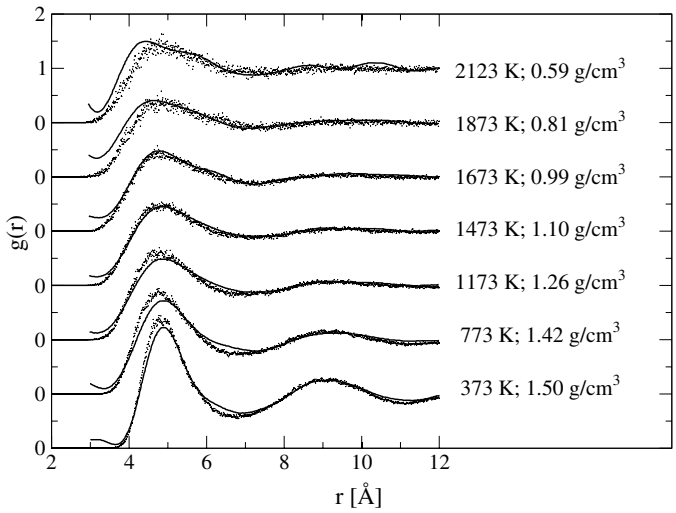

Figure 2. Pair correlation function for expanded fluid Rb: QMD simulations (data points) are compared with x-ray diffraction experiments (solid lines) [4]. The melting temperature at 1 bar is 312.2 K and the density of the solid is 1.52 g cm^{-3}. The critical point is located at 2017 K, 0.292 g cm^{-3}, and 124.5 bar [34].

coupling the electronic and ionic motion in the CP method is avoided in the present work because electronic and ionic timescales are decoupled when using the Born–Oppenheimer approximation.

From figures 1 and 2 one can see that the pair correlation functions derived from the QMD simulations are in good agreement with the experimental results. Therefore, the QMD method is capable of reproducing the structure of liquid Cs and Rb for a wide range of temperatures and

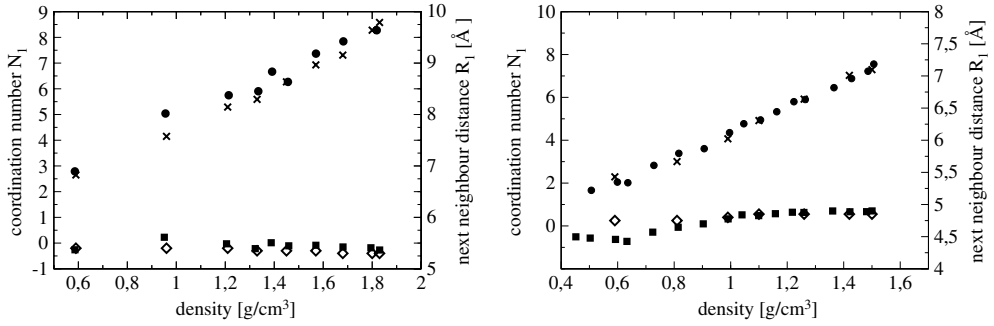

Figure 3. Coordination number and next-neighbour distance for expanded fluid Cs (left) and Rb (right). Full circles and boxes refer to experimental results, while crosses and open diamonds represent the respective QMD results.

densities from the melting to the critical point. A typical feature of the structural changes along the expansion of the liquid towards a gas is the decreasing maximum of the first and second peak. This transition has been treated as a bond network problem within a reverse Monte Carlo algorithm [35]. At high densities and low temperatures the bond network is dense with a high coordination number N_1. The next-neighbour distance R_1 stays almost constant decreasing the density and increasing the temperature along the liquid vapour coexistence line because clustering occurs and some atoms keep highly coordinated. The coordination number N_1 drops due to an increase of the number of atoms at the cluster surfaces, from about 8 (Cs) and 7 (Rb) at the melting point to about 3 (Cs) and 2 (Rb) at the lowest densities near the critical point. This bond network explains on an atomic level the steady decrease of N_1 at an almost constant R_1 as the density decreases both for Cs and Rb; see figure 3.

At densities lower than 1.0 g cm^{-3} the pair correlation functions for Rb displayed in figure 2 show a slight change of the shape at the first and second peak. This has been related to the onset of dimerization in liquid Rb [4]. The formation of dimers and further small neutral and charged clusters in expanded liquids and dense low-temperature plasmas has been predicted in advanced chemical models for the equation of state and the composition for a long time; see [5–7]. Earlier QMD simulations have shown evidence for the occurrence of Rb trimers rather than dimers under those conditions [25]; see also the discussion in section 4.

The deviations between the QMD results and the experimentally determined pair correlation functions for Cs shown in figure 1 are increasing along the expansion. These deviations are more pronounced than in the case of Rb. Of course, the pioneering neutron scattering experiments for expanded fluid Cs [2] did not have the precision of the x-ray diffraction experiments performed recently for Rb [4]. Another possible explanation is the relative high atomic number of Cs which makes it necessary to include relativistic corrections in the PP systematically. Another difference between these two liquids is the ionization energy, which is smaller for Cs than for Rb. This causes a more drastic transition from the metallic liquid to an atomic gas. The treatment of atomic states in the vapour is in principle difficult using plane wave codes like VASP which were originally developed for periodic systems at bulk densities.

4. Density of states and electron density

Besides the structural information, electronic properties such as the density of states (DOS) and the electronic charge density can also be extracted from the QMD simulations. We show as an

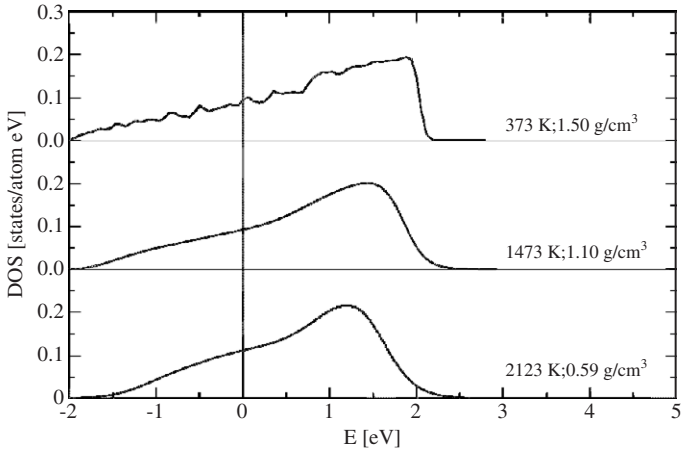

Figure 4. Density of states in Rb for three states along the expansion. The vertical line indicates the Fermi energy.

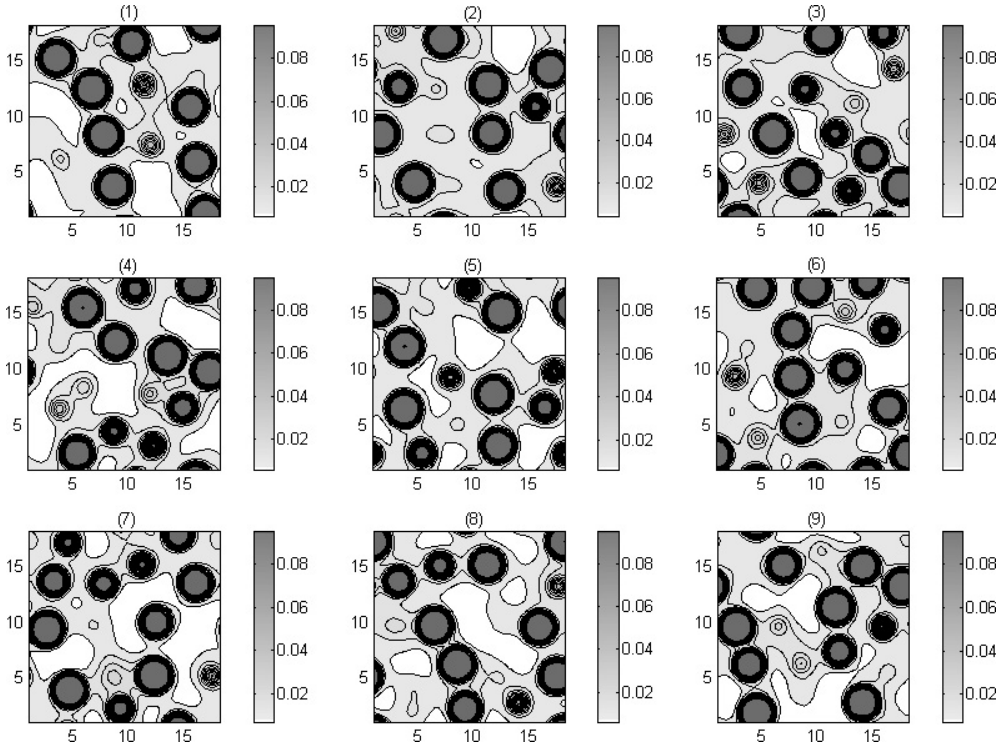

Figure 5. Contour plots of the electronic charge density in Rb near the melting point at 373 K and 1.5 g cm^{-3} along nine equidistant planes in the simulation cell from the top (1) to the bottom (9). The x- and y-axes of the planes are given in Å, and the colour code for the charge density is shown in units of e Å^{-3}.

example the change of the DOS in Rb from conditions near the melting point to the critical point region in figure 4. Although we have taken into account 32 points in the Brillouin zone

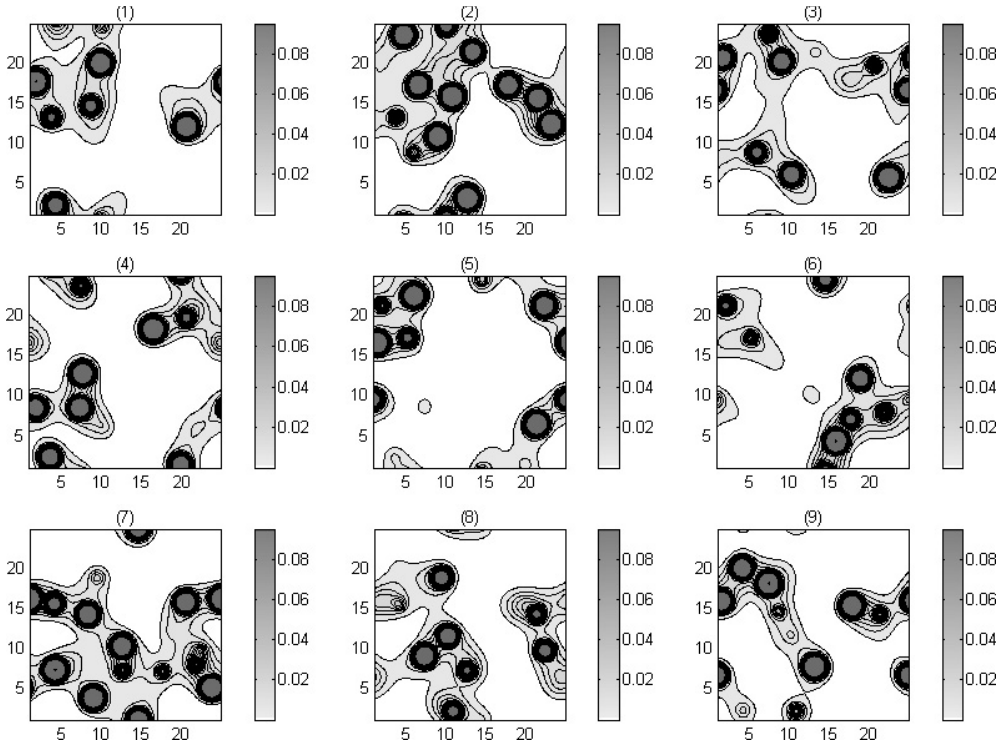

Figure 6. The same as in figure 5 but for conditions near the critical point of Rb at 2123 K and 0.59 g cm^{-3}.

for these calculations, small numerical fluctuations around the nearly-free-electron behaviour still occur in the DOS near the melting point. The maximum of the DOS relative to the Fermi energy is shifted from 1.9 to 1.2 eV, and the band edge is smeared out along the expansion. We can only identify a slight tendency to form a minimum just above the Fermi energy. The formation of two subbands separated by a pseudogap as a precursor for a metal-to-nonmetal transition is likely to appear at still lower densities.

Furthermore, we show contour plots of the electronic charge density in Rb for the two limiting cases near the melting (figure 5) and critical point (figure 6), respectively (compare also [21, 25]). These snapshots represent the charge density in the simulation cell along nine equidistant planes from the top (1) to the bottom (9) for a typical equilibrium configuration. One can see immediately that the electron charge density becomes strongly inhomogeneous with even large voids near the critical point compared with a rather smooth distribution near the melting point. The formation of two- and three-particle clusters is obviously favoured near the critical point, indicating that transient dimers and trimers occur. This trend is in agreement with the behaviour of the coordination number shown in figure 3 and the results of [25].

This behaviour of the DOS and of the electronic charge density indicates a localization of electrons at nuclei with decreasing density. Subsequently, a transition from a metallic to a nonmetallic state occurs which manifests itself in a strong decrease of the electrical conductivity in the region near the critical point as found experimentally, for example, for Cs [36]. Such a behaviour has been predicted by advanced chemical models [7]. In QMD simulations the electrical conductivity can be gained by evaluating the Kubo–Greenwood formula; see [17–19] for details. This is the subject of future work.

5. Conclusions

We have performed extensive QMD simulations for expanded fluid Cs and Rb. The agreement of the calculated pair correlation functions with experimental results is good for Rb and reasonable for Cs. The theoretical coordination numbers and next-neighbour distances follow the experimentally determined trends along the expansion. This behaviour can be explained within a bond-network problem [35]. A special feature is the formation of transient dimers or trimers such as Rb_2 and Rb_3 which possibly occurs already in the expanded fluid near the critical point, in agreement with earlier predictions of advanced chemical models [5, 6] and other QMD simulations [25]. The DOS and electronic charge density extracted from the QMD simulations show qualitatively the transition from a metallic to a nonmetallic state along the thermal expansion of the liquid from the melting point to the region of the critical point. How accurately QMD simulations can reproduce the experimentally known equation of state data including the location of the critical point [34] is an interesting future line of work.

Acknowledgments

We thank the authors of [4] for providing us with their data for Rb prior to publication. This work was supported by the Deutsche Forschungsgemeinschaft within the SFB 652 *Strong Correlations and Collective Phenomena in Radiation Fields*. The simulations were performed at the Norddeutscher Verbund für Hoch- und Höchstleistungsrechnen (HLRN) under account number mvp00006.

References

[1] Hensel F and Warren W W Jr 1999 *Fluid Metals* (Princeton, NJ: Princeton University Press)
[2] Winter R, Hensel F, Bodensteiner T and Gläser W 1987 *Ber. Bunsenges. Phys. Chem.* **91** 1327–30
[3] Pilgrim W-C, Ross M, Yang L H and Hensel F 1997 *Phys. Rev. Lett.* **78** 3685–8
[4] Matsuda K, Inui M, Niwa H, Mukaimoto S, Tada H and Tamura K 2005 *J. Non-Cryst. Solids* submitted
[5] Redmer R and Röpke G 1989 *Contrib. Plasma Phys.* **29** 343–53
[6] Redmer R and Warren W W Jr 1993 *Phys. Rev.* B **48** 14892–906
[7] Redmer R, Reinholz H, Röpke G, Winter R, Noll F and Hensel F 1992 *J. Phys.: Condens. Matter* **4** 1659–69
[8] Kahl G and Kambayashi S 1994 *J. Phys.: Condens. Matter* **6** 10897–921
[9] Kahl G 1994 *J. Phys.: Condens. Matter* **6** 10923–37
[10] Munejiri S, Shimojo K, Hoshino K and Watabe M 1997 *J. Phys.: Condens. Matter* **9** 3303–12
[11] Munejiri S, Shimojo F and Hoshino K 2000 *J. Phys.: Condens. Matter* **12** 4313–26
[12] Chihara J 1986 *Phys. Rev.* A **33** 2575–82
[13] Chihara J 1991 *J. Phys.: Condens. Matter* **3** 8715–44
[14] Chihara J and Kahl G 1998 *Phys. Rev.* B **58** 5314–21
[15] Gomez S, Gonzales L E, Gonzales D J, Stott M J, Dalgic S and Silbert M 1999 *J. Non-Cryst. Solids* **250–252** 163–7
[16] Mattsson A E, Schultz P A, Desjarlais M P, Mattsson T R and Leung K 2005 *Modelling Simul. Mater. Sci. Eng.* **13** R1–31
[17] Desjarlais M P, Kress J D and Collins L A 2002 *Phys. Rev.* E **66** 025401(R)
[18] Clérouin J, Renaudin P, Laudernet Y, Noiret P and Desjarlais M P 2005 *Phys. Rev.* B **71** 064203
[19] Desjarlais M P 2003 *Phys. Rev.* B **68** 064204
[20] Cabral B J C and Martins J L 1995 *Phys. Rev.* B **51** 872–7
[21] Shimojo F, Zempo Y, Hoshino K and Watabe M 1995 *Phys. Rev.* B **52** 9320–9
[22] Shimojo F, Zempo Y, Hoshino K and Watabe M 1997 *Phys. Rev.* B **55** 5708–11
[23] Hoshino K and Shimojo F 1996 *J. Phys.: Condens. Matter* **8** 9315–9
[24] Tsuji K, Katayama Y, Morimoto Y and Shimomura O 1996 *J. Non-Cryst. Solids* **205–207** 295–8
[25] Alemany M, Martins J and Cabral C 2004 *J. Non-Cryst. Solids* **347** 100–5
[26] Mermin N 1965 *Phys. Rev.* **137** A1441–3

[27] Kresse G and Hafner J 1993 *Phys. Rev.* B **47** 558–61
[28] Kresse G and Furthmüller J 1996 *Phys. Rev.* B **54** 11169–86
[29] Kresse G and Hafner J 1994 *Phys. Rev.* B **49** 14251–69
[30] Kresse G and Furthmüller J 1996 *Comput. Mater. Sci.* **6** 15–50
[31] Vanderbilt D 1990 *Phys. Rev.* B **41** 7892–5
[32] Kresse G and Hafner J 1994 *J. Phys.: Condens. Matter* **6** 8245–57
[33] Wang Y and Perdew J P 1991 *Phys. Rev.* B **44** 13298–307
[34] Jüngst S, Knuth B and Hensel F 1985 *Phys. Rev. Lett.* **55** 2160–3
[35] Nield V M, Howe M A and McGreevy R L 1991 *J. Phys.: Condens. Matter* **3** 7519–25
[36] Noll F, Pilgrim W C and Winter R 1988 *Z. Phys. Chem. Neue Folge* **156** 303–7